PHYSICAL REVIEW B **83**, 180405(R) (2011)

# Orbital occupation and magnetism of tetrahedrally coordinated iron in $CaBaFe_4O_7$

N. Hollmann,[1,2] M. Valldor,[1] Hua Wu,[1] Z. Hu,[2] N. Qureshi,[1] T. Willers,[1] Y.-Y. Chin,[1,2] J. C. Cezar,[3] A. Tanaka,[4] N. B. Brookes,[3] and L. H. Tjeng[2]

[1]*II. Physikalisches Institut, Universität zu Köln, Zülpicher Str. 77, D-50937 Köln, Germany*

[2]*Max Planck Institute for Chemical Physics of Solids, Nöthnitzerstr. 40, D-01187 Dresden, Germany*

[3]*European Synchrotron Radiation Facility, Boîte Postale 220, F-38043 Grenoble Cédex, France*

[4]*Department of Quantum Matter, ADSM, Hiroshima University, Higashi-Hiroshima 739-8530, Japan*

(Received 22 November 2010; revised manuscript received 7 February 2011; published 3 May 2011)

$CaBaFe_4O_7$ is a mixed-valent transition metal oxide having both $Fe^{2+}$ and $Fe^{3+}$ ions in tetrahedral coordination. Here we characterize its magnetic properties by magnetization measurements and investigate its local electronic structure using soft x-ray absorption spectroscopy at the Fe $L_{2,3}$ edges, in combination with multiplet cluster simulations and band structure calculations. We found that the $Fe^{2+}$ ion in the unusual tetrahedral coordination is Jahn-Teller active with the high-spin $e^2_\uparrow t^3_{2\uparrow} e^1_\downarrow$ configuration having a minority-spin electron with an $x^2$-$y^2$ character. We deduce that there is an appreciable orbital moment of $L_z \approx 0.36$ caused by multiplet interactions, thereby explaining the observed magnetic anisotropy.

DOI: 10.1103/PhysRevB.83.180405 PACS number(s): 75.25.Dk, 75.30.Gw, 71.70.Ej, 71.70.Ch

Transition-metal oxides are well known for their strongly correlated electronic structure that brings orbital, spin, and lattice degrees of freedom into close interaction.[1] The resulting phenomena, among them high $T_C$ and unconventional superconductivity, colossal magneto resistance, and various kinds of magnetic and orbital order, have been mostly studied in perovskites.[2] Recently, the material $CaBaFe_4O_7$ was synthesized,[3] belonging to the class of *Swedenborgites* or "114" oxides.[4–6] It is a mixed-valent system containing equal numbers of $Fe^{2+}$ and $Fe^{3+}$ ions. Both ions are tetrahedrally coordinated by oxygen atoms. This tetrahedral coordination is especially rare for $Fe^{2+}$, and has been studied mainly in sulfites.[7–9] The Fe ions in $CaBaFe_4O_7$ constitute a sublattice of alternating kagomé and trigonal layers as shown in Fig. 1(a). The shorter average Fe-O distances[10] observed in the trigonal layers indicate the accommodation of only $Fe^{3+}$ ions, leaving the kagomé layers with a 2 : 1 ratio of $Fe^{2+}$ and $Fe^{3+}$ ions. It is not clear whether charge ordering is present in these kagomé layers.

The 3*d* orbitals in a tetrahedral $FeO_4$ coordination are split into a low *e* and a high $t_2$ level, and the $Fe^{2+}$ ion in the high-spin state has an $e^2_\uparrow t^3_{2\uparrow} e^1_\downarrow$ configuration. As one minority-spin electron resides in the twofold degenerate *e* orbital, the question arises whether or not this degeneracy will be lifted, and if so, which orbital is to be occupied. The presence of such Jahn-Teller active[11,12] ions could lead to interesting orbital physics phenomena, influencing strongly the magnetic properties of the material.[13,14] In this work, we characterize the magnetic properties of $CaBaFe_4O_7$ by magnetization measurements and study the orbital occupation and the local magnetism of the Fe ions using a combination of soft x-ray absorption spectroscopy (XAS) and multiplet cluster calculations, supported by additional spin-resolved band structure calculations.

We have succeeded to grow high-quality single crystals of $CaBaFe_4O_7$ using the floating zone method.[10] The XAS experiments were performed at the ID08 beam line at the ESRF in Grenoble, France. The energy resolution was $\approx 0.25$eV at the Fe-$L_{2,3}$ edge, with a degree of linear and circular polarization each higher than 99%. The single crystals were cleaved *in situ* in ultrahigh vacuum in the low $10^{-10}$ mbar range. The Fe-$L_{2,3}$ XAS spectra were taken in total electron yield mode. Polycrystalline $Fe_2O_3$ was measured simultaneously as a reference. A high-field magnet with $B = 5$ T was used to measure the magnetic circular dichroism (XMCD) in XAS. The magnetic susceptibility has been measured during warming up using a vibrating sample magnetometer in a Physical Properties Measurement System of Quantum Design.

Single crystal diffraction measurements yield an orthorhombic structure ($Pbn21$), with lattice parameters 6.3135, 11.0173, and 10.3497 Å.[10] The magnetic susceptibility in Fig. 1(b) shows a strong rise at 270 K, indicating magnetic ordering similar to the data measured on polycrystalline samples.[3] Additionally, the single crystal data display a cusp at 200 K, indicating a second magnetic transition. In a recent neutron scattering study,[10] a change in the magnetic ordering pattern was found at this temperature. The differences between field- and zero-field-cooled measurements are small, indicating the absence of magnetic degeneracy. The data also show a clear anisotropy with a magnetic easy *c* axis. The magnetic ordering has been described as ferrimagnetic.[3] The strong pinning of the moments along the *c* axis seems surprising, as one would expect that the high-spin Fe ions with their half-filled $t_2$ shell ($Fe^{3+}$ $e^2t_2^3$ and $Fe^{2+}$ $e^3t_2^3$) should not carry an orbital moment. Yet we will show below that the spin-orbit coupling (SOC) via multiplet interactions can generate an appreciable orbital moment, thereby explaining the observed magnetic anisotropy. For what it is worth, a Curie-Weiss fit of the inverse susceptibility in the 320- to 350-K range gives an effective moment of 2.1 $\mu_B$ and a Curie temperature of 295 K [see Fig. 1(c)]. Isothermal magnetization data are shown in Fig. 1(d). The size of the magnetic moments is consistent with the results from polycrystalline samples.[15]

Figure 2 shows the Fe-$L_{2,3}$ XAS spectra of $CaBaFe_4O_7$ taken with the **E** vector parallel and perpendicular to the *c* axis. The top panel displays the spectra taken at 300 K, in the paramagnetic phase, while the bottom panel depicts the spectra at 100 K, in the magnetically ordered phase. There is

 ©2011 American Physical Society

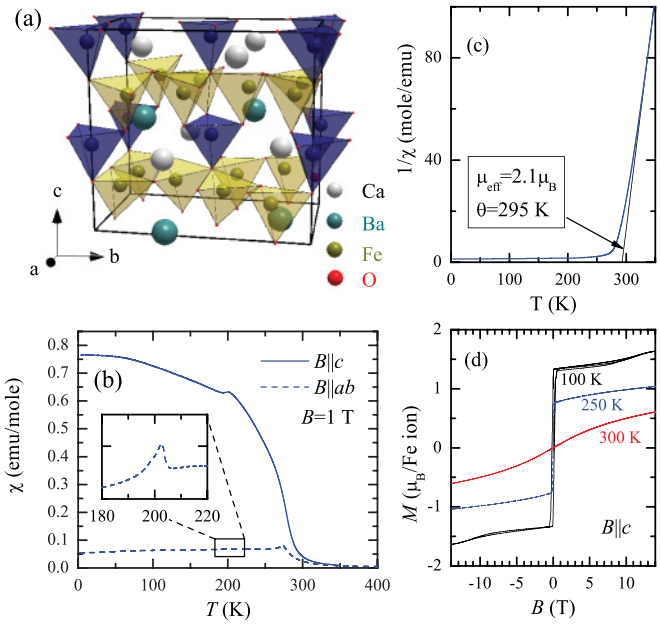


FIG. 1. (Color online) (a) A sketch of the crystal structure, with the $FeO_4$ tetrahedra in the kagomé layer (yellow/light gray) and in the trigonal layer (blue/dark gray). (b) Magnetic susceptibility, (c) inverse susceptibility, and (d) isothermal magnetization.

a distinct polarization dependence, which is more pronounced for the magnetically ordered phase. The difference between the two polarizations, labeled XLD (x-ray linear dichroism), is also plotted.

The spectra in Fig. 2 are dominated by the Fe $2p$ core-hole SOC which splits the spectrum roughly in two parts, namely the $L_3$ ($h\nu \approx 705$–$713$ eV) and $L_2$ ($h\nu \approx 718$–$725$ eV) *white line* regions. The line shape strongly depends on the multiplet structure given by the Fe $3d$-$3d$ and $2p$-$3d$ Coulomb and exchange interactions, as well as by the local crystal fields and the hybridization with the O $2p$ ligands. Unique to soft XAS is that the dipole selection rules are very sensitive in determining which of the $2p^5 3d^{n+1}$ final states can be reached and with what intensity, starting from a particular $2p^6 3d^n$ initial state ($n = 5$ for $Fe^{3+}$ and $n = 6$ for $Fe^{2+}$).[16–18] This makes the technique extremely sensitive to the symmetry of the initial state, for example, the crystal field states of the ions.

The $L_{2,3}$ XAS process is furthermore charge sensitive, and the spectra of higher valencies appear at higher photon energies by about 1 eV per electron count difference.[19,20] We may therefore expect that the low-energy shoulder of the $L_3$ white line at 708 eV is due to predominantly the $Fe^{2+}$, while the higher energy peak at 709 eV comes from the $Fe^{3+}$. These assignments are in fact consistent with the XLD observations. It is known that XLD can have its origin in an anisotropy of the orbital occupation and/or spin orientation of the ions under study.[18,21] For a $Fe^{3+}$ ion, however, the spherical ${}^6A_1$ high-spin $3d^5$ configuration can only produce a significant XLD if macroscopically there is a net spin axis present.[22] Therefore, the absence of XLD for the 709-eV peak ($\sim Fe^{3+}$) at 300 K and its appearance at 100 K indicate the magnetic ordering of the $Fe^{3+}$ ions in going from 300 to 100 K.

To check the above assignments, we performed quantitative simulations of the XAS spectra with the XTLS 8.3 program

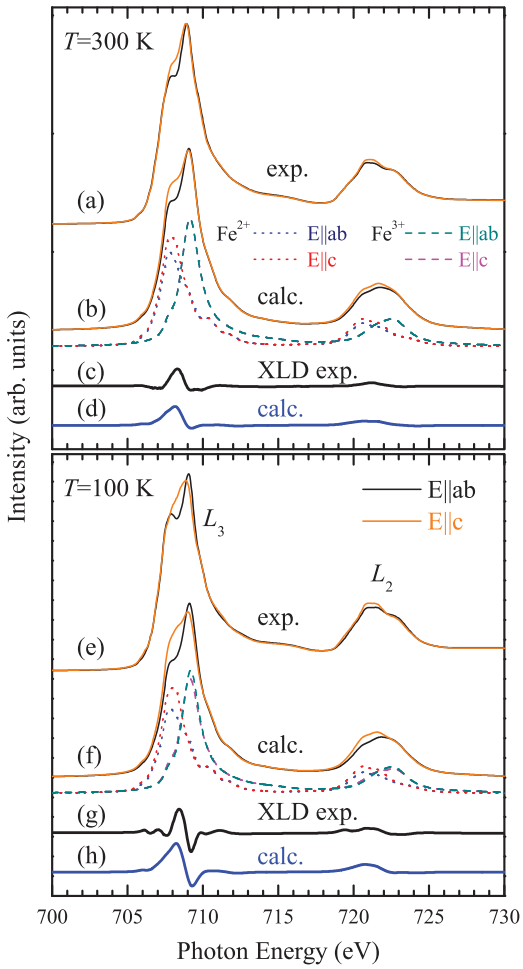


FIG. 2. (Color online) Experimental and calculated Fe $L_{2,3}$ XAS spectra of $CaBaFe_4O_7$ with linear polarized light.

using a configuration-interaction cluster model including full atomic-multiplet theory.[16–18] The multipole parts of Coulomb interaction and the single-particle SOC constant $\zeta$ were estimated from Hartree-Fock values that were reduced to 80%. For the monopole parts of the Coulomb interaction $U_{dd}$ and $U_{pd}$, and the charge-transfer energy $\Delta$, typical values were used;[17,23] the Fe-O hybridization was estimated with the Slater-Koster formalism[24] and Harrison's description[25], assuming different Fe-O distances for each ion, with 1.85 Å for $Fe^{3+}$ and 1.94 Å for $Fe^{2+}$.[10] Spectra of $Fe^{2+}$ and $Fe^{3+}$ were calculated separately and added in an incoherent sum in a ratio of 1:1.

The results for the simulations are displayed in Fig. 2. One can observe good overall agreement between experiment and calculation: each individual spectrum is well reproduced, that is, for each of the two polarizations as well as for both temperatures 300 and 100 K. The XLD is also well described. The simulations confirm that the $L_3$ white line at 708 eV is due to the $Fe^{2+}$, while the 709 eV peak comes from the $Fe^{3+}$, and that the two ions have indeed a ratio of 1:1, indicative of the oxygen content being close to seven. We now discuss the origin of the polarization dependence and its implications for the orbital occupation and spin orientation.

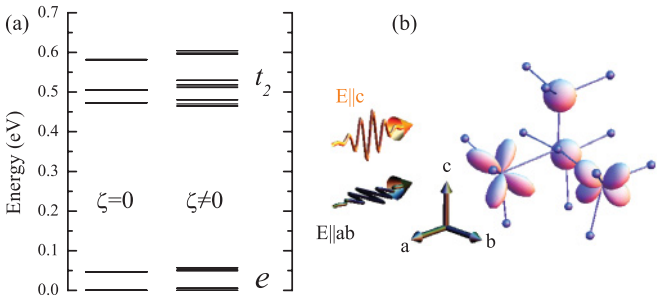


FIG. 3. (Color online) (a) Total-energy level diagram for the $Fe^{2+}$ ion, excluding (left) and including (right) the Fe $3d$ SOC. (b) An illustration of the minority spin $x^2$-$y^2$ orbital of the $Fe^{2+}$ ion; the high-spin $3d^5$ $Fe^{3+}$ ion is drawn as a sphere.

We start with the 300-K spectrum in which the high-spin $Fe^{3+}$ ion with its spherical $^6A_1$ $3d^5$ configuration does not contribute to the linear dichroism since there is no magnetic ordering at this temperature. The polarization dependence is then caused by the $Fe^{2+}$ ion only and is related to its anisotropic orbital occupation. This is revealed in Fig. 3(a), where we display the total-energy level diagram of the $Fe^{2+}$ ion. Looking first at the calculation in which we artificially switch off the $3d$ SOC $\zeta$, we find that there is a Jahn-Teller splitting of the $e$ and $t_2$ manifolds. The lowest state has an $e^2_\uparrow t^3_{2\uparrow} e^1_\downarrow$ configuration with the minority-spin $e$ electron occupying the local $x^2$-$y^2$ orbital [see Fig. 3(b)]. The first excited state has a $3z^2$-$r^2$-like symmetry and lies 50 meV higher, that is, it will only be slightly occupied at 300 K. Thus the $2p \rightarrow 3d$ XAS intensity is slightly higher for $\mathbf{E} \| c$ than for $\mathbf{E} \| ab$.

We have checked this order of energy levels by carrying out band structure calculations in the local-spin-density approximation using the WIEN2K code[26] and the single-crystal diffraction data.[10] Specifically, we have set up an impurity calculation by introducing one substitutional $Mn^{2+}$ ion into one of the $Fe^{2+}$ sites in the kagomé plane. This charge neutral substitution facilitates the interpretation since $Mn^{2+}$ has the high-spin closed $3d^5$ shell configuration that will not lead to possibly complex interorbital interactions as is in the case of $Fe^{2+}$. We have then determined the centers of gravity of the various orbitally resolved partial densities of states of the Mn ion. The result is that the lowest lying $3d$ orbital is of the $x^2$-$y^2$ type, with a $3z^2$-$r^2$ orbital state lying about 50 meV higher energy. These calculations thus support our spectroscopic analysis described above.

The orbital character of the minority-spin electron in the $e$ level is not purely $x^2$-$y^2$: Two effects provide mixing with other orbitals. First, SOC mixes $t_2$ character into the $e$ levels. This can be seen in the energy-level diagram where multiplets that are degenerate without SOC [Fig. 3(a); $\zeta = 0$] are split up [Fig. 3(a); $\zeta \neq 0$]. Second, mixing of orbital character is also caused by the low local symmetry at the $Fe^{2+}$ site as the $FeO_4$ tetrahedra are distorted with a symmetry lower than $T_d$.

In analyzing the spectra in the magnetically ordered phase at $T = 100$ K in Fig. 2(e), we find that the experimental XLD changes slightly at the position of the $Fe^{2+}$ and that an additional dichroism is created at the $Fe^{3+}$ $L_3$ peak. This is related to the x-ray magnetic linear dichroism (XMLD) that is induced by the magnetic ordering.[27] In addition, the XMLD effect not only depends on the orientation of the magnetic moment with respect to the polarization, but also on the local coordination.[28] The XMLD for $Fe^{3+}$ can be reproduced by assuming the moments to be canted by $\approx 35^\circ$ away from the $c$ axis, as seen in Figs. 2(f) and 2(h). The orbital occupation is hardly affected by the magnetic ordering.

We have carried out XMCD measurements of the Fe-$L_{2,3}$ edge, which probe directly the local magnetism of the Fe ions.[29–31] The external magnetic field was parallel to the $c$ axis. The temperature dependence of the XMCD signal [Figs. 4(e)–4(g)] follows clearly the magnetic susceptibility in Fig. 1(b), with a strong increase in XMCD signal upon cooling below the first transition at 270 K, and a further increase in the second ordered phase at 100 K.[32] Here, we can also make use of the charge sensitivity of the XAS process: The XMCD signal at around 708 eV is mostly of $Fe^{2+}$ character, the signal at 709 eV mostly of $Fe^{3+}$ character. Both signals have an opposite sign, indicating an antiparallel alignment of the moments. From the small XMCD signal at 709 eV we can conclude that the two $Fe^{3+}$ moments, one in the kagomé and the other in the trigonal plane, do not compensate and yield a small net moment. Their net moment opposes the $Fe^{2+}$ net moment.

Full-multiplet calculations have also been carried out to analyze the XMCD data, using the same parameters as for the XLD. The results are shown in Figs. 4(d) and 4(h). The agreement with the experiment is very satisfactory, ensuring an accurate understanding of the local electronic structure of the Fe ions. This allows us to extract the spin and orbital

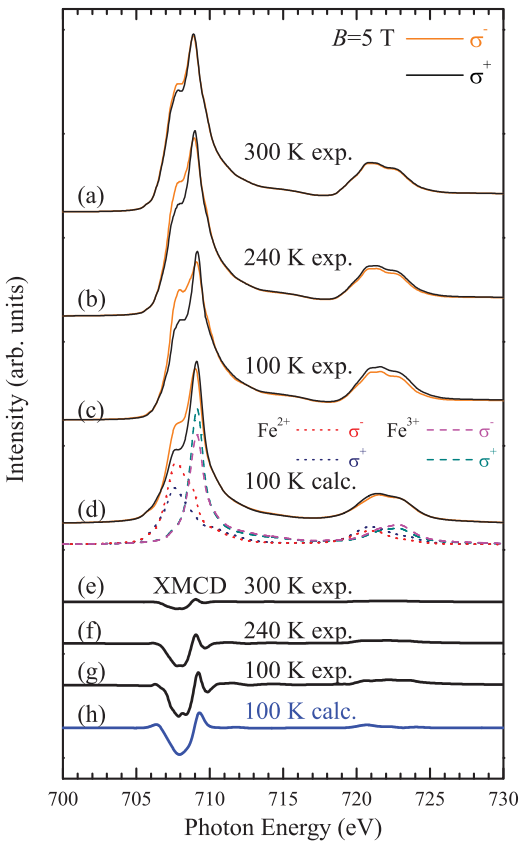


FIG. 4. (Color online) X-ray magnetic circular dichroism of $CaBaFe_4O_7$.

contributions to the local magnetic moment. Along the easy axis, the expectation value of the spin for the $Fe^{2+}$ ions is $S_z = 1.9$, that is, close to the spin-only value of two. Interestingly, the $Fe^{2+}$ ions each have also an additional orbital moment of $L_z = 0.36$. This is caused by the SOC mixing of the $e$ and $t_2$ orbitals, which is not negligible as their energy separation is rather small in tetrahedral coordination as compared to octahedral coordination. The local distortion may cause a pronounced single ion anisotropy. As different $Fe^{2+}$ sites have their respective easy magnetic axes, canting of their magnetic moments occurs due to these anisotropies.

In conclusion, we have analyzed the orbital occupation and local magnetism of the tetrahedrally coordinated Fe ions in $CaBaFe_4O_7$ with x-ray absorption spectroscopy. By means of full-multiplet cluster simulations of the x-ray linear dichroism, we deduce that the $Fe^{2+}$ with its high-spin $e^3t_2^3$ orbital occupation undergoes an $e$ Jahn-Teller distortion which stabilizes a local $x^2$-$y^2$ orbital state. The local distortion of the $FeO_4$ tetrahedra and the spin-orbit coupling mix some $t_2$ character into this $x^2$-$y^2$ state, which induces an orbital moment, explaining the magnetic anisotropy observed in the bulk magnetic measurements. A "ferrimagnetic" alignment of the magnetic moments was proposed based on the x-ray magnetic circular dichroism.

We gratefully acknowledge the European Synchrotron Radiation Facility staff for providing us with beam time. This work is supported by the DFG via SFB 608. N.H. and T.W. are also supported by the Bonn-Cologne Graduate School.

[1] N. Tsuda, K. Nasu, A. Yanase, and K. Siratori, *Electronic Conduction in Oxides*, Springer Series in Solid-State Sciences 94 (Springer Verlag, Berlin, 1991).

[2] M. Imada, A. Fujimori, and Y. Tokura, Rev. Mod. Phys. **70**, 1039 (1998).

[3] B. Raveau, V. Caignaert, V. Pralong, D. Pelloquin, and A. Maignan, Chem. Mater. **20**, 6295 (2008).

[4] M. Valldor and M. Andersson, Solid State Sci. **4**, 923 (2002).

[5] M. Valldor, Solid State Sci. **6**, 251 (2004).

[6] B. Raveau, V. Caignaert, V. Pralong, and A. Maignan, Z. Anorg. Allg. Chem. **635**, 1869 (2009).

[7] M. S. Park, S. K. Kwon, S. J. Youn, and B. I. Min, Phys. Rev. B **59**, 10018 (1999).

[8] A. Krimmel, M. Mücksch, V. Tsurkan, M. M. Koza, H. Mutka, and A. Loidl, Phys. Rev. Lett. **94**, 237402 (2005).

[9] S. Sarkar, T. Maitra, R. Valentí, and T. Saha-Dasgupta, Phys. Rev. B **82**, 041105 (2010).

[10] N. Qureshi *et al.* (unpublished); See supplemental material at [http://link.aps.org/supplemental/10.1103/PhysRevB.83.180405] for the structural data.

[11] H. A. Jahn and E. Teller, Proc. R. Soc. London A **161**, 220 (1937).

[12] H. A. Jahn, Proc. R. Soc. London A **164**, 117 (1938).

[13] K. I. Kugel and D. I. Khomskii, Sov. Phys. Usp. **25**, 231 (1982).

[14] Y. Tokura and N. Nagaosa, Science **288**, 463 (2000).

[15] K. Vijayanandhini, Ch. Simon, V. Pralong, V. Caignaert, and B. Raveau, Phys. Rev. B **79**, 224407 (2009).

[16] F. M. F. de Groot, J. Electron Spectrosc. Relat. Phenom. **67**, 529 (1994).

[17] A. Tanaka and T. Jo, J. Phys. Soc. Jpn. **63**, 2788 (1994).

[18] See the "Theo Thole Memorial Issue," J. Electron Spectrosc. Relat. Phenom. **86**, 1 (1997).

[19] C. T. Chen and F. Sette, Phys. Scr. T **31**, 119 (1990).

[20] C. Mitra, Z. Hu, P. Raychaudhuri, S. Wirth, S. I. Csiszar, H. H. Hsieh, H.-J. Lin, C. T. Chen, and L. H. Tjeng, Phys. Rev. B **67**, 092404 (2003).

[21] S. I. Csiszar, M. W. Haverkort, Z. Hu, A. Tanaka, H. H. Hsieh, H.-J. Lin, C. T. Chen, T. Hibma, and L. H. Tjeng, Phys. Rev. Lett. **95**, 187205 (2005).

[22] P. Kuiper, B. G. Searle, P. Rudolf, L. H. Tjeng, and C. T. Chen, Phys. Rev. Lett. **70**, 1549 (1993).

[23] Parameters for $Fe^{3+}$ [eV]: $U_{dd} = 5.0$, $U_{pd} = 6.0$, $\Delta = 1$; for $Fe^{2+}$: $U_{dd} = 6.5$, $U_{pd} = 8.0$, $\Delta = 5$.

[24] J. C. Slater and G. F. Koster, Phys. Rev. **94**, 1498 (1954).

[25] W. Harrison, *Electronic Structure and the Properties of Solids* (Dover, New York, 1989).

[26] P. Blaha, K. Schwarz, G. Madsen, D. Kvasnicka, and J. Luitz, [http://www.wien2k.at/].

[27] P. Kuiper, B. G. Searle, P. Rudolf, L. H. Tjeng, and C. T. Chen, Phys. Rev. Lett. **70**, 1549 (1993).

[28] E. Arenholz, G. van der Laan, R. V. Chopdekar, and Y. Suzuki, Phys. Rev. Lett. **98**, 197201 (2007).

[29] B. T. Thole, P. Carra, F. Sette, and G. van der Laan, Phys. Rev. Lett. **68**, 1943 (1992).

[30] P. Carra, B. T. Thole, M. Altarelli, and X. Wang, Phys. Rev. Lett. **70**, 694 (1993).

[31] C. T. Chen, Y. U. Idzerda, H.-J. Lin, N. V. Smith, G. Meigs, E. Chaban, G. H. Ho, E. Pellegrin, and F. Sette, Phys. Rev. Lett. **75**, 152 (1995).

[32] No significant change in XMCD line shape was found when going across the transition at 200 K, indicating that the transition is not connected to the local magnetism but is caused by long-range effects.